The effect of nitriding, severe shot peening and their combination on the fatigue behavior and micro-structure of a low-alloy steel

S.M. Hassani-Gangaraj [a], A. Moridi [a], M. Guagliano [a,*], A. Ghidini [b], M. Boniardi [a]

[a] Politecnico di Milano, Dipartimento di Meccanica, Via La Masa 1, 20156 Milano, Italy
[b] Lucchini RS S.p.A., Via G. Paglia, 45, 24065 Lovere, Italy

Article history:
Received 29 October 2012
Received in revised form 23 February 2013
Accepted 22 April 2013
Available online 2 May 2013

1. Introduction

Majority of failures in engineering materials such as fatigue fracture, fretting fatigue, wear and corrosion, are very sensitive to the structure and properties of the material surface, and in most cases failures originate from the exterior layers of the work piece. Therefore, it would be considerably effective to apply some technological process to enhance the material properties on the surface of the part.

It is well established that the fatigue strength of mechanical components can be enhanced by producing compressive residual stress, increasing the hardness and reducing the grain size. Mechanical treatments such as shot peening and thermo-chemical treatments such as nitriding are extensively used to improve fatigue, corrosion and wear resistance. Shot peening is mostly benefited by generating compressive residual stress and nitriding is mostly benefited by increasing the hardness. Both processes, nonetheless, can be benefited by the additional effect. That is to say, shot peening can also increase the hardness and nitriding is also able to produce compressive residual stress, even if there might be some doubts on the introduction of high level compressive residual stress. A positive synergistic effect, therefore, could be anticipated if these two processes are combined. In order to take the advantage of the third factor, i.e. reducing the grain size shot peening can be performed by severe parameters. While a lot of effort was made in the last four decades to reveal the manner of residual stress generation during shot peening and its effect on fatigue life, it has not been a long time that shot peening was recognized as a potential process to produce surface nano-crystallizations. The common aspect is to use special combinations of peening parameters to multiply the kinetic energy of the shot impacts in order to generate a large number of defects, dislocations and interfaces (grain boundaries) on the surface layer of treated part and consequently transform its micro-structure into ultra-fine grains or nano-structure [1]. In this case, the process is called severe shot peening rather than shot peening to emphasize the obtained micro-structural refinement at surface layers.

While there is a solid background in the literature that both shot peening and nitriding can improve fatigue behavior, their combination is less investigated. In this regard, literature can be classified into two main groups. Some researcher applied shot peening after nitriding and some other studied the reverse process:

* Corresponding author. Tel.: +39 02 23998206; fax: +39 02 23998202.
E-mail address: mario.guagliano@polimi.it (M. Guagliano).

1.1. Nitriding followed by shot peening

Freddi et al. [2] performed nitriding on 32CrMoV13 steel specimens and subsequently subjected them to shot peening, varying shot diameter and Almen intensity in two levels. Slight improvement of fatigue limit (5–10%) depending on the peening parameters was reported for combined treatment as compared to nitriding. Croccolo et al. [3] subjected unnotched and notched 32CrMoV13 steel specimens to shot peening after nitriding. No significant enhancement of fatigue limit (only 3%) with respect to the nitrided-only specimens was reported for smooth specimens. Rolling contact fatigue behavior of the same steel was investigated after deep nitriding and following shot peening. Following shot peening could prolong rolling contact fatigue life and make the spalled pit lower and smaller [4]. Contact fatigue test performed on carbo-nitrided-only and carbo-nitrided plus shot peened gears made of AISI 4130 steel showed that damage to the gears appears after about the same testing time for both kinds of treatments but in different forms: pitting and spalling for the carbo-nitrided-only gears and micro-pitting for the carbo-nitrided and shot peened gears [5]. This combination was not always beneficial. Deterioration of surface durability during sliding rolling contact fatigue behavior of maraging steel subjected to nitriding and fine particle peening was also reported in the literature [6].

Fernandez Pariente et al. [7] Investigated the effect of nitriding plus shot peening on fatigue strength of a low alloy steel specimens containing a micro-hole, acting as a pre-crack. The threshold value of stress intensity factor increased from 14.2 MPa $m^{1/2}$ for nitrided specimen to 25.1 MPa $m^{1/2}$ for nitrided plus shot peened specimens. Terres et al. investigated the effect of nitriding and the following shot peening on bending fatigue behavior of 42CrMo4 steel. More improvement (35%) for fatigue limit was obtained by nitriding plus shot peening with respect to the nitrided-only specimens (8%). This was mentioned to be due to the hardened layer that retarded the initiation of a fatigue crack by constraining the plastic deformation [8].

1.2. Shot peening prior to nitriding

The idea here is that by increasing the grain boundary area and dislocation density, enhanced diffusion could be expected in ultrafine grained and nano-structured surface layers. That is to say in this case shot peening can be useful only if performed with more severe parameters with respect to the conventional ones, thus becoming a severe plastic deformation process.

It was shown that radio frequency plasma nitriding of stainless steel in combination with a pre-treatment by high pressure torsion results in an enhanced thickness of the nitrided layer and increased surface hardness [9]. The reason was mentioned to be the transformation of the coarse grained structure into a very fine grained one as a result of high pressure torsion. The same result was also reported by applying shot peening prior to plasma nitriding of stainless steel [10]. In addition to dislocation density increment, in this case strain induced transformation of austenite to martensite had beneficial effects to provide faster diffusion. Application of shot peening to produce plastic deformation at the near surface layer of AISI 304 austenite stainless steel before plasma nitriding led to twice thicker nitrided layer than not peened specimens and improved hardness down to a deeper region from the surface under the same plasma nitriding condition [11]. Wear resistance and corrosion behavior of nitrided 316L austenitic steel can be enhanced by employing shot peening before gas nitriding [12].

Tong et al. [13] affirmed the possibility of performing nitriding at lower temperature (300 °C) for pure iron samples by generating nano-structured surface layers through a prior surface mechanical attrition (SMAT). The much depressed nitriding temperature is attributed to enhanced nitrogen diffusion in the nano-crystalline surface layer relative to the coarse grains. It was also found that the SMAT iron sample developed a nitrided layer twice as thick as that on a coarse-grained sample under the same gaseous nitriding conditions [14].

Kikuchi et al. [15] applied fine particle peening prior to gas nitriding of AISI 316 austenitic stainless steel notched specimens. The micro-hardness values for the nitrided-only specimens were the same as that of untreated specimen. On the other hand much higher micro-hardness values were achieved by application of fine particle peening prior to nitriding. This hybrid treatment could also improve the fatigue strength as compared to nitriding. However, the fatigue strength of double treated specimens was not substantially higher than fine particle peened specimens.

In the light of this literature review, it can be concluded that regarding the fatigue strength there are few studies carried out to clarify the effect of shot peening prior to nitriding. Indeed most of these studies concerned about the capability of this combination to increase subsequent nitriding diffusion layer and surface hardness. In the case of performing shot peening after nitriding the published result is somehow controversial. Minor, major and even no considerable improvement have been reported and it is not clear when someone could expect the best. Moreover, the effect of shot peening and nitriding combination on micro-structural changes was not widely investigated. Above all, it is not yet known which sequence of this combination leads to the best results if fatigue behavior is concerned. It is therefore the purpose of this study to clarify these unexplored aspects of nitriding and shot peening combination.

In the present study severe shot peening, nitriding and their combination, considering both sequences, have been performed on steel specimens. The treated specimens have been characterized by optical and scanning electron microscopy (SEM) observation, residual stress measurement using X-ray diffraction (XRD), micro-hardness tests and surface roughness measurement. The specimens have been tested through rotating bending fatigue tests performed at room temperature. SEM observations of the fractured surfaces along with a local fatigue strength approach was applied to justify the experimental results.

2. Materials and methods

The material used in this study was low-alloy steel ESKYLOS6959. Its chemical composition is summarized in Table 1. Mechanical properties evaluated through tension test are the following: 878 MPa yield stress, 1010 MPa ultimate tensile strength and 17.7% elongation at break. Rotating bending fatigue test specimens were machined from a forging according to the extraction map provided in Fig. 1a. The forging was quenched from 880 °C in water and then tempered at 635 °C for 5 h. The specimen geometry is presented in Fig. 1b.

Five batches containing 12 specimens per each batch were prepared to obtain rotating bending fatigue limit in order to compare the effects of various surface treatments on the fatigue behavior of the studied material. Different batches with corresponding naming conventions are classified in Table 2. The first group is as-received. Second and third groups were subjected to nitriding and severe shot peening respectively. Nitriding followed by severe shot peening was applied for the fourth batch. The last group was subjected to severe shot peening prior to nitriding.

Standard steel shots S230, using an air blast machine were employed to conduct severe shot peening. The shot peening intensity measured on "Almen A" strip was 18A. Shot peening was performed with 1000% coverage to ensure surface layers are severely

Table 1
Chemical composition of steel grade 1.6959 used in this study (wt.%).

C	Mn	Si	Cr	Mo	Al	Ni	V	S	P
0.28–0.3	0.6–0.65	0.30–0.35	0.83–0.88	0.51–0.54	0.02–0.035	3–3.1	0.09–0.12	0.003	0.015

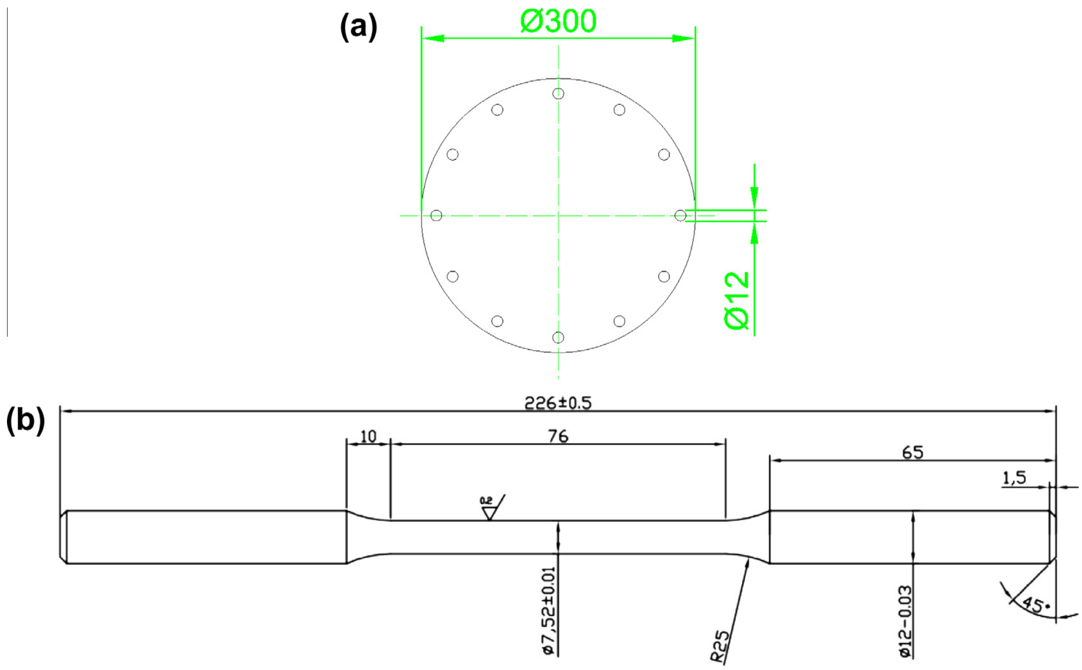

Fig. 1. (a) Extraction map of rotating bending fatigue specimens. (b) The detailed specimen geometry used for rotating bending fatigue test. All dimensions are given in mm.

Table 2
Specimens naming convention.

Group name	Description
AR	As-Received
N	Nitrided
SSP	Severe Shot Peened
N + SSP	Nitrided plus Severe Shot Peened
SSP + N	Severe Shot Peened plus Nitrided

deformed. Gas nitriding was carried out in an industrial unit. Processing temperature and time were 510 °C and 15 h respectively.

Cross sections of the samples were prepared by a standard grinding, polishing and etching procedure and micro-structure observations were performed using Zeiss EVO50 SEM with thermionic source and optical microscopy. Specimens for OM and SEM observations have been etched by 5% Nital. Micro-hardness measurements have also been performed on specimen's section respectively. A diamond Vickers indenter was used, applying a maximum force of 100 gf. The load was applied gradually at a constant 0.1 Ns^{-1} rate with a dwell time of 15 s. Three measurements were performed at each depth and averaged to account for measurement errors and material's heterogeneity. The resultant data scattering was not more than 10%.

To study the state of residual stresses and to obtain a more precise distribution of hardening, XRD analysis of the surface layer in the treated specimens was performed using an AST X-Stress 3000 X-ray diffractometer (radiation Cr Kα, irradiated area 3.14 mm^2, $\sin^2\psi$ method, diffraction angle (2θ) ~156 scanned between −45 and 45). Fig. 2a shows the specimen during XRD analysis of residual stress. In depth measurements have been carried out step by step by removing a very thin layer of material (0.01–0.02 mm) using an electro-polishing device in order to obtain the in-depth profile of residual stresses. A solution of Acetic acid (94%) and Perchloric acid (6%) has been used for electro-polishing. On each specimen, material removal has been carried on up to the depth showing insignificant compressive residual stress values.

A Mahr profilometer PGK, that is an electronic contact instrument, equipped with MFW-250 mechanical probe and a stylus with tip radius of 2 μm was used to trace the surface profiles of treated specimens (shown in Fig. 2b). The acquired signal was then elaborated by Mahr Perthometer Concept 5 software [16] to obtain the standard roughness parameters. Surface roughness data were obtained by performing three measurements along three distinct 0.8 mm long surface axial lines of each individual specimen to consider the variability of surface roughness by location. The final reported experimental surface roughness values in the present work are the mean value of the three performed measurements.

Rotating bending fatigue tests (stress ratio $R = -1$) have been carried out at room temperature with a nominal frequency of 20 Hz for all batches. Staircase procedure [17] considering 10 MPa as step was followed to elaborate data and to calculate the fatigue limit. Rotating bending fatigue test machine is presented in Fig. 2c.

3. Results and discussion

3.1. Micro-structure

As demonstrated in Fig. 3, from the overall view of the cross section by optical microscopy three distinct regions can be recognized for all nitrided specimens. A very thin white (compound) layer of few microns was formed on the top surface. The composition of

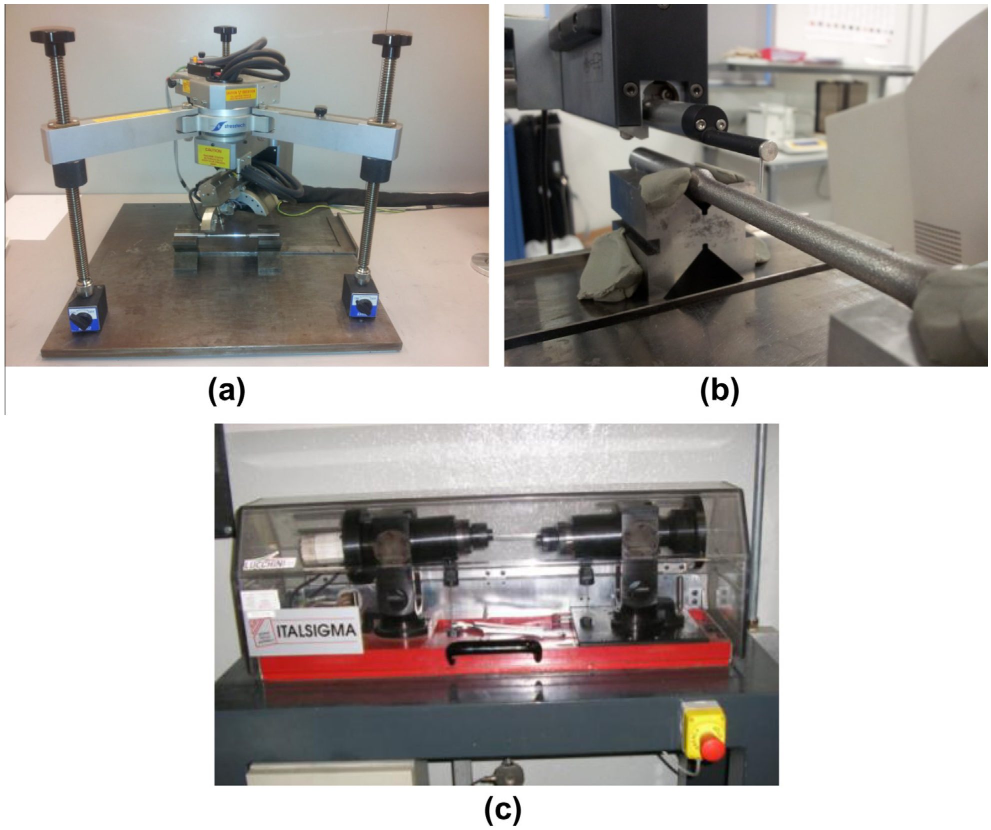

Fig. 2. The experimental setup for (a) XRD measurement of residual stress, (b) roughness parameters measurement and (c) rotating bending fatigue test.

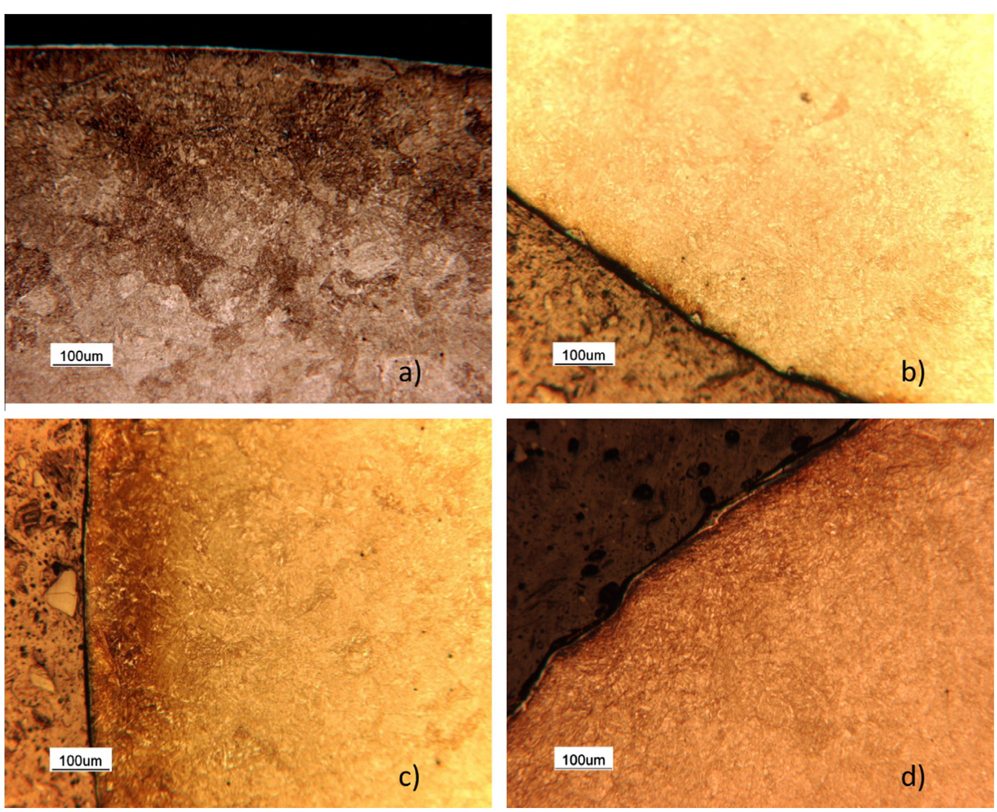

Fig. 3. Cross sectional optical microscopy of (a) N, (b) SSP, (c) N + SSP and (d) SSP + N specimens.

this hard and brittle layer is dependent on nitriding processing parameters. However, with the conventional processing parameters it is usually a combination of Υ' (Fe_4N) and ε ($Fe_{2-3}N$) phases. More information can be found in [18] on micro-structural evolution during nitriding. Beneath the compound layer the so called diffusion zone with dispersed needle shape precipitates of Υ' in ferritic matrix as well as the solid solution of nitrogen in ferrite exists. Compound and diffusion layer are considered as hardened case after nitriding. Below the diffusion layer, substrate without any evidences of micro-structural change can be observed. No micro-structural change can be observed for severe shot peened specimen through optical microscopy.

Fig. 4 illustrates scanning electron microscopy of the cross section of the treated specimens. Formation of compound layer after nitriding is more evident here (Fig. 4a). Depth of compound layer was measured to be in the range of 4–6 μm after nitriding. A precise look at the top surface of the nitrided specimen demonstrates that pores have been formed up to 1–2 μm within the compound layer (shown with arrows).

Subsequent severe shot peening suppressed the porous structure at the top of the compound layer (Fig. 4c). The rest of compound layer, on the other hand, survived after peening. Nonetheless, it was highly damaged and lots of micro-cracks (shown with arrows) were formed. Formation of micro-cracks can be explained by considering high brittleness of compound layer and high coverage applied for shot peening. Bearing in mind that 1000% coverage, theoretically, means each part of the surface has been treated at least ten times with steel shots. When such a hard and brittle layer is subjected to repeated impingements, possibility of micro-crack formation increases.

Performing severe shot peening prior to nitriding caused up to three times deeper compound layer (Fig. 4d) with respect to the nitrided-only specimen. This is due to the very dense structure and fine grained surface layer generated by severe plastic deformation during severe shot peening (Fig. 4b). A clear micro-structure change can be observed at the top surface layers of severe shot peened specimen up to 10–12 μm. By severe shot peening much more defects and interfaces are generated in surface layers through repeating impingements. With the proceeding of collisions, some areas approach to the critical condition of nanocrystallization and grain fragmentation below 100 nm occurs [1]. In fact, in conventional nitriding of coarse-grained steel, nitrogen diffusion in the Fe lattice dominates. In the nano-crystalline structures, on the other hand, nitrogen mostly diffuses along grain boundaries with much faster diffusivity because of a much smaller activation energy (approximately half) compared with that for the lattice diffusion [13]. It is also worth mentioning here that the compound layer in this case is not as dense as nitrided or nitrided plus severe shot peened specimen and more porosity and even some discontinuity can be observed in the upper part of the compound layer.

3.2. Hardening

Fig. 5 depicts the variation of micro-hardness from the treated surface to the bulk material. Maximum value of micro-hardness was measured at the surface of all treated specimens and then it gradually decreased to the core value. It is worth to notice that hardness improvement by severe shot peening, even if it is a severe plastic deformation process, was by far lower than nitriding.

Case depth after nitriding is a matter of convention. Technically it is defined to be the depth at which the hardness is 100 HV more than the core hardness [19]. A hardness value of 10% above the core hardness has been also used in the literature to characterize the case depth after nitriding when the fatigue characteristics are regarded [20,21]. Therefore, this value was also superimposed in the graph of Fig. 5. According to this criterion the case depth after nitriding was measured to be approximately 500 μm. The combination of nitriding and severe shot peening, regardless of the sequence, did not change the hardened layer depth. Nonetheless, this combination did improve the micro-hardness from surface

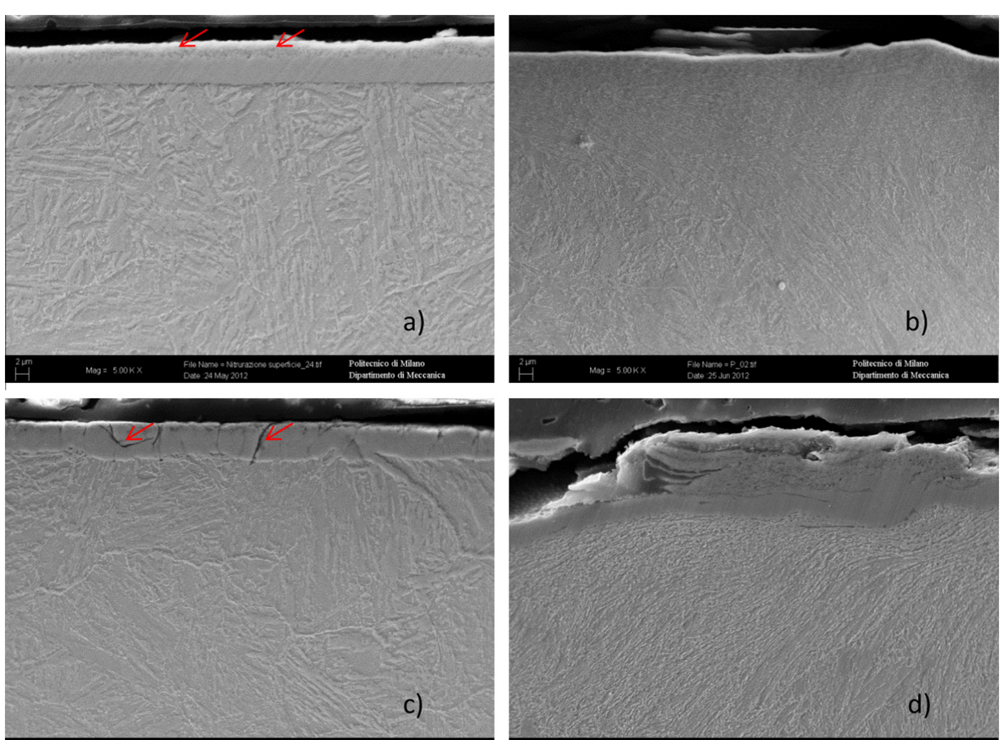

Fig. 4. Cross sectional scanning electron microscopy of (a) N, (b) SSP, (c) N + SSP and (d) SSP + N specimens.

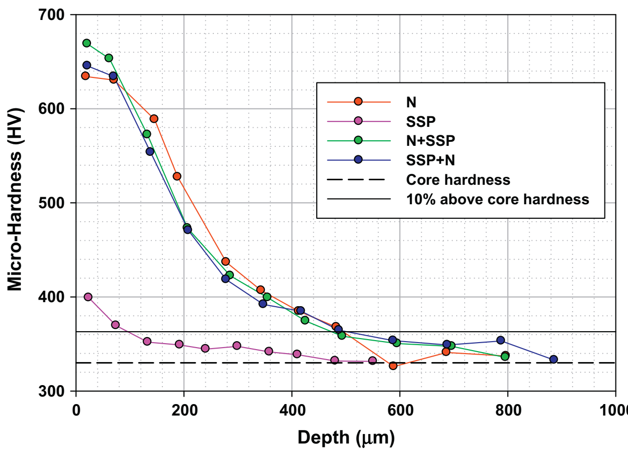

Fig. 5. In depth micro-hardness distribution of all surface treated specimens.

up to 80 μm in depth. The maximum surface hardness is obtained when sever shot peening is performed after nitriding.

It was shown that the width of the diffraction peak at half of the maximum (FWHM) measured by XRD is able to reflect more aspects of surface work hardening which cannot be revealed by micro-hardness values [7]. FWHM appears to interest the only layer where the measurement is done. On the contrary, micro-hardness involves a finite thickness of material, and the results are an average value on the thickness of material where the indentation has been done. FWHM is related to the grain distortion, to the dislocation density and grain size. It is also assumed as an index of hardening of the material.

The in-depth FWHM distribution of all treated specimens is illustrated in Fig. 6. The estimated depth of hardened layer by FWHM distribution is in a good agreement with that of obtained by micro-hardness distribution. Contrary to micro-hardness, near surface (up to 25 μm in depth) FWHM for severe shot peened specimen is higher than nitrided specimen. The reason is that severe shot peening can drastically deform surface layers and accumulate plastic strain due to repeated impingements.

The beneficial effect of severe shot peening and nitriding combination to generate harder surface layer can be realized from FWHM distribution. In the case of severe shot peening prior to nitriding this improvement might be attributed to facilitated nitrogen diffusion through dense structure and fine grained layers generated after severe plastic deformation. The most enhanced FWHM

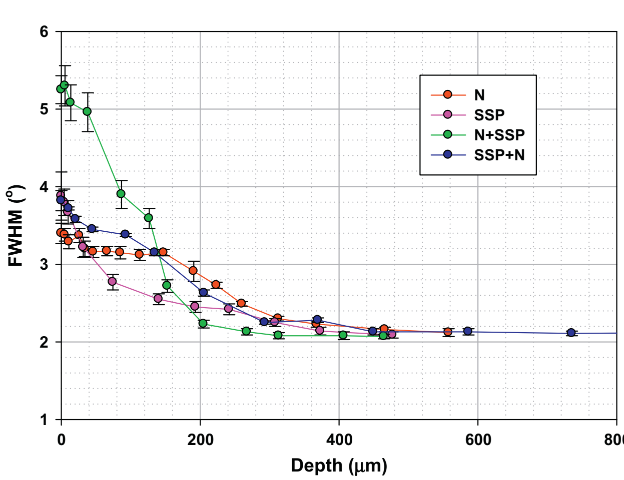

Fig. 6. In depth FWHM distribution of all surface treated specimens.

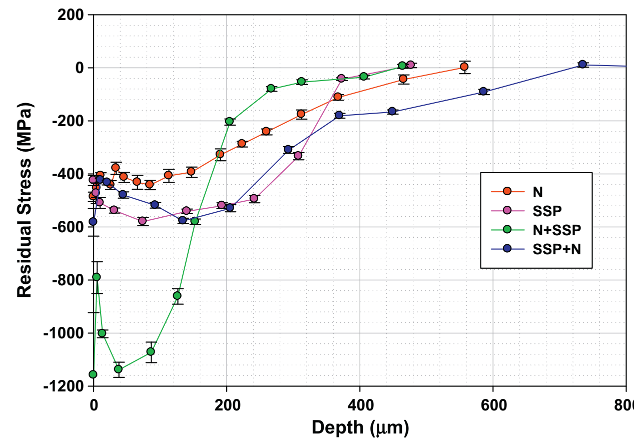

Fig. 7. In depth residual stress distribution of all surface treated specimens.

occurred in the reverse treatment (N + SSP), however. This is due to the fact that a very hard target has been subjected to severe peening.

3.3. Residual stress

In depth residual stress distribution of all treated specimens is depicted in Fig. 7. It should be mentioned that both longitudinal and circumferential residual stresses were measured. For all treated specimen the state of stress was quite equibiaxial. Thus one component of residual stress (longitudinal) was plotted here. Severe shot peening generated more compressive residual stress than nitriding. Indeed, both processes increase hardness and generate compressive residual stress. However, based on the result of this study, nitriding is mostly benefitted by increasing the hardness while shot peening is mostly benefited by generating compressive residual stress.

The combination of nitriding and shot peening can be advantageous in terms of residual stress distribution. In the case of severe shot peening prior to nitriding, deeper compressed layer is produced as compared to the only nitriding. In the case of severe shot peening after nitriding, on the other hand, remarkable augmentation is achieved for surface and maximum compressive residual stress. Distribution of residual stress then is followed by a steeper reduction in this case with respect to the nitrided specimen.

3.4. Surface roughness

Table 3 shows the surface roughness parameters of all treated specimens. The parameters are based on the definition of ISO 4287 [22]. The arithmetic-mean value (R_a) can be considered as the representative parameter of surface roughness. It is interesting to note that nitriding increased the roughness, even if it is not a mechanical treatment. This increment in the nitrided specimen can be attributed to the formation of pores at the top of the compound layer.

Table 3
Surface roughness parameters of all treated specimens.

Treatment	l_r (mm)	l_n (mm)	R_a (μm)	R_q (μm)	R_z (μm)	R_t (μm)
AR	0.8	4	0.07	0.10	0.62	0.82
N	0.8	4	0.59	0.76	4.37	5.04
SSP	0.8	4	4.93	6.02	23.82	32.96
N + SSP	0.8	4	1.49	1.87	7.05	9.88
SSP + N	0.8	4	5.23	6.5	25.49	33.22

Severe shot peening has considerably increased the roughness. This is a well-recognized side effect of the shot peening process. Surface roughness of peened plus nitrided specimen is a little bit more than the roughness of peened specimen. This again affirms that nitriding alters the surface roughness. Surface roughness for nitrided plus peened specimen is not as high as the peened-only specimen. This is due to the fact that in the former case very hard nitrided layer was subjected to sever shot peening. Therefore, less deformation and eventually less surface roughness was generated.

3.5. Fatigue limit

Fig. 8 shows the fatigue limit for as-received and all surface treated specimens. Fatigue limit of as-received specimen was 491 MPa. Severe shot peening increased the fatigue limit of specimens by 11.6%. Surface roughness alteration, generation of compressive residual stresses, micro-structure refinement and slight improvement of hardness were the main effects induced by severe shot peening. It seems that the detrimental effect of surface roughness masked part of the potential improvement that could be resulted by severe shot peening.

Nitriding was able to significantly increase the fatigue limit by 51.3%. It will be shown in the next section that fatigue crack initiated form the subsurface layer of nitrided specimens. The difference between shot peening and nitriding improvement could be related to harder and much less rough surface of the nitrided specimen that caused the fatigue crack to be shifted to the subsurface where the applied bending stress is less than surface.

It is worth to notice that the fatigue limit of the combined shot peened and nitrided specimens, regardless of sequence, was almost the same as the fatigue limit of nitrided specimen. Despite the initial expectation of having a synergistic effect of the combination of these surface treatments, no further improvement in fatigue limit was obtained with respect to the nitrided-only specimen. A justification is presented in the following sections.

3.6. Fractography

The fractured surface of all treated specimens was examined by SEM observation to assess the effect of different surface treatments on fatigue crack initiation and propagation. Fig. 9a shows the fractured surface of a nitrided specimen. The final fracture resulted from initiation and propagation of a subsurface, so-called "fish eye" crack. It should be noted that fish eye crack feature has been observed in all broken nitrided specimens. The same fracture mechanism for nitrided specimen has been also reported elsewhere [23,24]. Bearing in mind that specimens were subjected to rotating bending loading condition, surface layers were exposed to more severe applied stress than subsurface layers. However, fatigue crack has not originated from the surface. Indeed, crack initiation site was below the hardened layer produced by nitriding. Depth of hardened layer measured by micro-hardness test was around 500 μm and depth of compressed layer measured by XRD was approximately 550 μm. The depth of crack initiating site for nitrided specimens was extended up to 762 μm. This observation confirms that high hardness and compressive residual stress generated by nitriding made a great delay in surface crack initiation. It is well accepted that extrusion and intrusion pile up is responsible for crack initiation on the surface. However, in nitrided specimen extrusion and intrusion process is very limited by surrounding hard material and they could not be easily piled up [25].

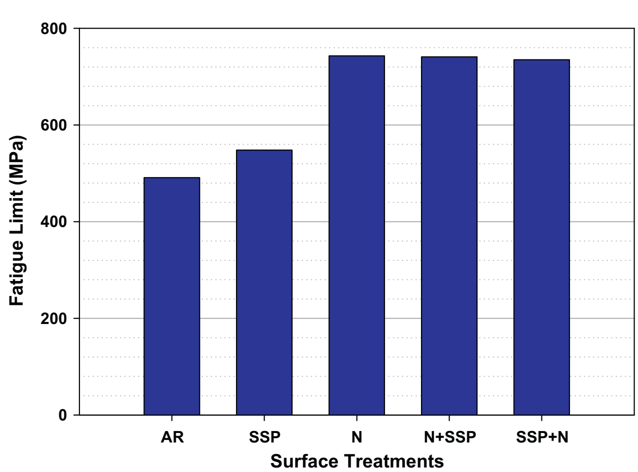

Fig. 8. Fatigue limit of as-received and surface treated specimens.

The same fish eye crack feature, as illustrated in Fig. 9b and c was observed for both combinations of severe shot peening and nitriding, in all broken specimens except one SSP + N specimen. The depth of crack initiation sites for N + SSP and SSP + N were in the range of 565–819 μm and 521–847 μm respectively. It is the result of interest that notwithstanding the presence of surface micro-crack in the compound layer of N + SSP or high surface roughness as well as some discontinues in the compound layer of SSP + N, the fatigue crack still originated from the subsurface layers in both cases. Indeed, the high compressive residual stress field prevented micro-cracks and discontinuities to be further propagated.

For the severe shot peened specimens, on the other hand, fatigue crack initiated from the surface (Fig. 9d). Considering the existence of ultra-fine grained layer and high compressive residual stresses in the surface layers, the crack was also in this case expected to initiate from subsurface layers. Nonetheless, it seems that the deteriorating effect of high surface roughness on fatigue resistance has masked partly the beneficial effect of ultra-fine grained structures containing high compressive residual stress. Fractured surface of severe shot peened specimens also revealed multiple crack initiation sites feature on the surface. This is a typical feature of fatigue fracture not in smooth but in notched specimens. Bearing in mind that the tested specimens were smooth, it can be concluded that high surface roughness induced by severe shot peening acted like a notch during the fatigue test.

3.7. Local fatigue strength

Hardness and residual stress are two important parameters governing the fatigue behavior of steel. Local fatigue strength approach correlates the local fatigue strength to the hardness and residual stress distribution. This approach is most often applied for surface hardened material [15,26,27]. Local fatigue approach proposed by Kloos and Velten [28] is implemented in this study but similar results are obtained if other local fatigue limit formulations are used. Local fatigue (σ_w), is considered to be a function of base fatigue limit (σ_{w0}), ultimate tensile strength (R_m), induced micro-hardness (HV), residual stress (σ_{res}), mean applied stress (σ_m), as well as applied relative stress gradient (X^*) by the following relationships:

$$R_m = 3.29\,\mathrm{HV} - 47 \quad \mathrm{HV} \leqslant 445 \tag{1}$$

$$R_m = 4.02\,\mathrm{HV} - 374 \quad \mathrm{HV} \succ 445 \tag{2}$$

$$\sigma_{w0} = 1.27\,\mathrm{HV} + 150 \quad \mathrm{HV} \leqslant 500 \tag{3}$$

$$\sigma_{w0} = 785 \quad \mathrm{HV} \succ 500 \tag{4}$$

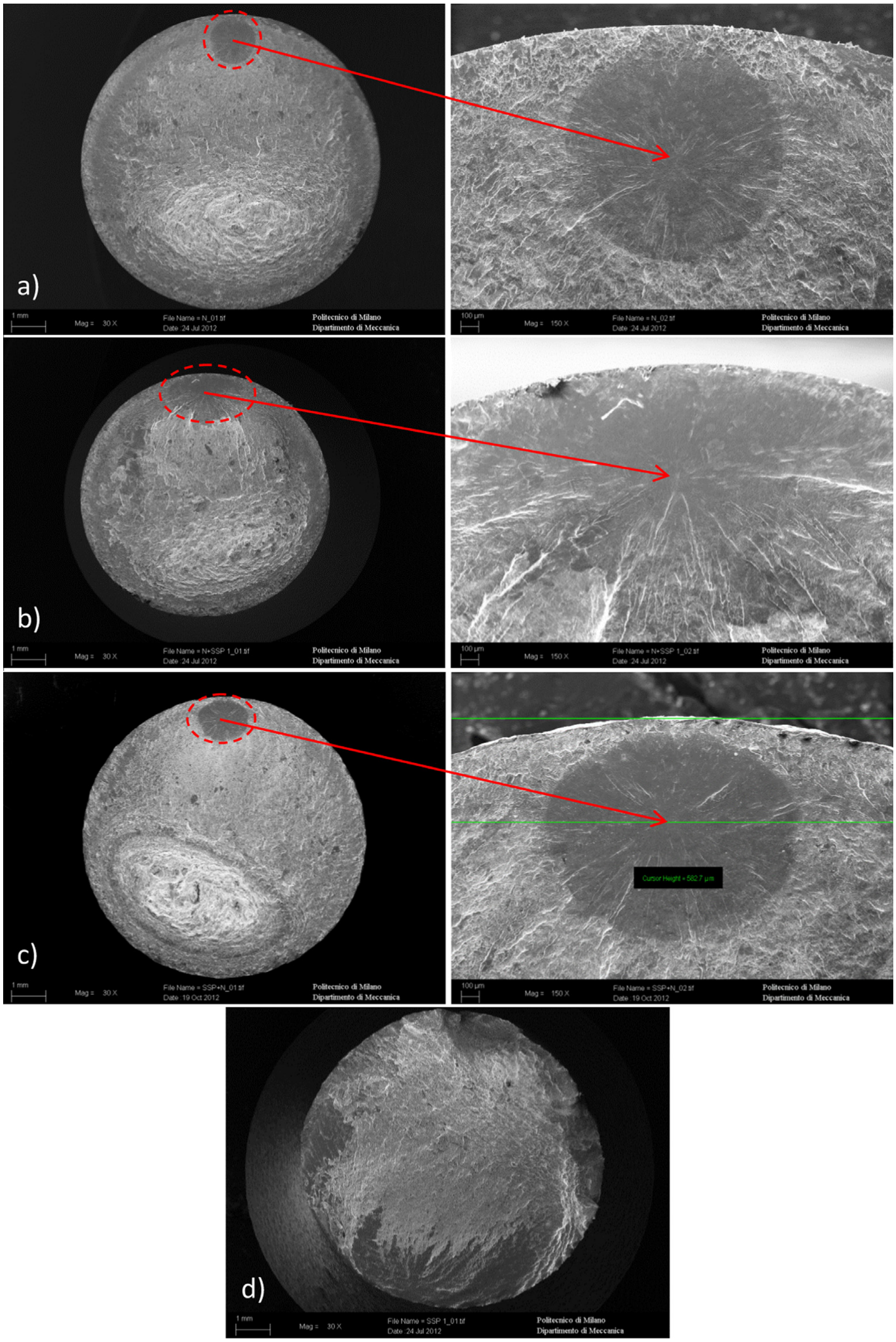

Fig. 9. SEM fractography of surface treated samples: (a) N, (b) N + SSP, (c) SSP + N and (d) SSP.

$$X^{*} = \frac{1}{\sigma_{\max}} \cdot \frac{d\sigma}{dx} \tag{5}$$

$$\sigma_w = \sigma_{w0}\left(1 - \frac{\sigma_m + \sigma_{res}}{R_m}\right)\left(1 + \sqrt{\frac{1600}{\mathrm{HV}^2} X^{*}}\right) \tag{6}$$

The local fatigue strength curves of all treated specimens are depicted in Fig. 10. Straight lines represent stress distribution for different levels of applied bending stress. The intersection of applied stress distribution with local fatigue curve represents the predicted site of crack initiation and its corresponding surface value indicates the predicted nominal fatigue limit by this method. It can be seen that theoretically fatigue cracks are most likely to initiate at the depth of 500–800 μm for all treated specimens. This is in a good agreement with experimental observation for N, N + SSP and SSP + N series. However, for severe shot peened specimens, unlike the prediction, all fatigue cracks initiated from the surface. This is due to high surface roughness induced by severe shot peening. It should

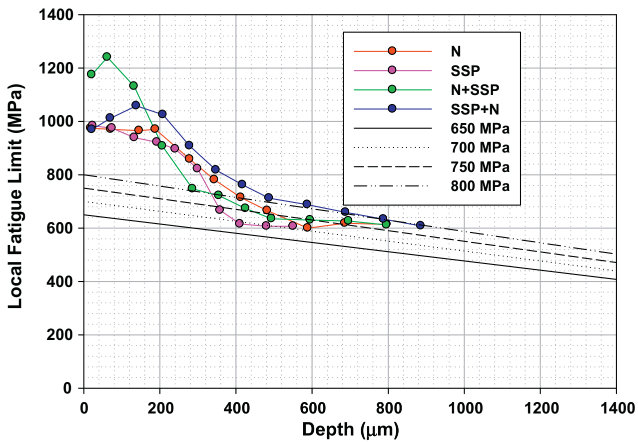

Fig. 10. Local fatigue strength of surface treated specimens.

be reminded that the effect of surface roughness is not taken into account in the presented local fatigue strength approach. It is worth mentioning that despite almost the same surface roughness values for SSP and SSP + N, fatigue crack initiated from the surface in the former case and from the subsurface layer in the latter case. This observation affirms the capability of the nitriding process to delay fatigue crack initiation phase by increasing the surface hardness. The calculated fatigue limits are also in a good agreement with the measured ones for N, N + SSP and SSP + N series.

The fact that despite the increment in compressive residual stress and work hardening, subsequent or prior severe shot peening has not improved the fatigue limit of nitrided specimens can be clearly explained by distribution of local fatigue limit shown in Fig. 10. High Improvement due to subsequent severe shot peening occurred at the surface and subsurface layers up to approximately 200 μm in depth. In the case of prior severe shot peening, major improvement occurred at subsurface layers up to the depth of 300 μm. Notwithstanding the crack initiation in the depth of 500 μm or even deeper, these further improved regions by hybrid treatments were already safe enough regions by single nitriding where the intersection of applied stress and local fatigue curve does not occur. Accordingly, for the smooth specimens to achieve further fatigue life improvement, nitriding should be combined with a treatment that is able to affect deeper than nitrided hardened layer. It is worth mentioning that in the case of notched specimens where stress gradient exists, fatigue cracks are most likely to initiate from the surface. Thus fatigue limit improvement can be expected when nitriding and severe shot peening is combined.

4. Conclusion

The effect of severe shot peening, nitriding and their combination considering both sequences (severe shot peening + nitriding and vice versa) on micro-structure, hardening, residual stress, surface roughness and fatigue limit of steel alloy was investigated. The following conclusions can be drawn on the basis of obtained results:

- Subsequent severe shot peening suppressed the porous structure at the top of the compound layer formed after nitriding. The rest of compound layer, on the other hand, survived after peening. Nonetheless, it was damaged and some micro-cracks were formed.
- Performing severe shot peening prior to nitriding caused up to three times deeper compound layer with respect to the nitrided-only specimen. This is due to the very dense structure and ultra-fine grained/nano-structured surface layer generated by severe plastic deformation during severe shot peening.
- Hardness improvement by severe shot peening, even if it is a severe plastic deformation, was by far lower than nitriding.
- The combination of nitriding and severe shot peening, regardless of the sequence, did not change the hardened layer depth. Nonetheless, this combination did improve the micro-hardness from surface up to 80 μm in depth. The maximum surface hardness is obtained when sever shot peening is performed after nitriding.
- The estimated depth of hardened layer by FWHM distribution is in a good agreement with that of obtained by micro-hardness distribution. Contrary to micro-hardness, near surface (up to 25 μm in depth) FWHM for Severe shot peened specimen is higher than nitrided specimen. This is due to drastically deformed surface layer after severe shot peening.
- In the case of severe shot peening prior to nitriding, deeper compressed layer is produced as compared to the only nitriding. In the case of severe shot peening after nitriding, on the other hand, remarkable augmentation is achieved for surface and maximum compressive residual stress.
- Even if nitriding is not a mechanical treatment, it increased the surface roughness (R_a) of as-received sample from 0.07 μm to 0.59 μm and roughness of the peened sample from 4.93 μm to 5.23 μm. Severe shot peening tremendously raised surface roughness.
- Notwithstanding the high surface roughness, severe shot peening improved the fatigue limit by 11.6%.
- Nitriding improved the fatigue limit by 51.3%. No further improvement was obtained by the combination of severe shot peening and nitriding.
- For nitrided series (N, N + SSP, SSP + N) fatigue crack originated from subsurface layers below the hardened layer. Fatigue crack initiation from the surface of severe shot peened specimens is attributed to the high induced surface roughness. Subsequent nitriding was able to displace the crack initiation site to the subsurface layers despite the presence of high surface roughness.
- With respect to nitrided-only specimens, the combination of severe shot peening and nitriding enabled to improve local fatigue limit up to 200 μm in depth for N + SSP and 300 μm for SSP + N. However, since almost all fatigue cracks were likely to initiate at the depth of 500–800 μm, this combination did not succeed to improve the final fatigue limit. In order to achieve further improvement on the fatigue limit of nitrided smooth specimen, this is a key factor, that nitriding should be combined with another surface treatment enabling to affect deeper than the hardened layer produced by nitriding.

Acknowledgments

The authors would like to thank Dr. Michele Bandini, for his contribution to this research and execution of shot peening in Peen Service srl. The authors would also like to thank Mr. Oscar Manella for his help with performing fatigue tests.

References

[1] M. Guagliano, in: S. Baiker (Ed.), Shot peening, A dynamic application and its future, 3rd edition Wetzikon, 2012, Metal Finishing News, Chapter 16th: Severe Shot Peening to Obtain Nanostructured Surfaces: Processes, Properties and Application.

[2] Freddi A, Veschi D, Bandini M, Giovani G. Design of experiments to investigate residual stresses and fatigue life improvement by a surface treatment. Fatigue Fract Eng M 1997;20:1147–57.

[3] Croccolo D, Cristofolini L, Bandini M, Freddi A. Fatigue strength of shot-peened nitrided steel: optimization of process parameters by means of design of the experiment. Fatigue Fract Eng M 2002;25:695–707.

[4] Gao YK. Influence of deep-nitriding and shot peening on rolling contact fatigue performance of 32Cr3MoVA steel. J Mater Eng Perform 2008;17:455–9.
[5] Batista AC, Dias AM, Lebrun JL, Le Flour JC, Inglebert G. Contact fatigue of automotive gears: evolution and effects of residual stresses introduced by surface treatments. Fatigue Fract Eng M 2000;23:217–28.
[6] Ohue Y, Matsumoto K. Sliding-rolling contact fatigue and wear of maraging steel roller with ion-nitriding and fine particle shot-peening. Wear 2007;263: 782–9.
[7] Fernandez Pariente I, Guagliano M. About the role of residual stresses and surface work hardening on fatigue ΔKth of a nitrided and shot peened low-alloy steel. Surf Coat Technol 2008;202:3072–80.
[8] Terres MA, Laalai N, Sidhom H. Effect of nitriding and shot-peening on the fatigue behavior of 42CrMo4 steel: experimental analysis and predictive approach. Mater Des 2012;35:741–8.
[9] Ferkel H, Glatzer M, Estrin Y, Valiev RZ. RF plasma nitriding of a severely deformed high alloyed steel. Scr Mater 2002;46:623–8.
[10] Ji SJ, Wang L, Sun JC, Hei ZK. The effects of severe surface deformation on plasma nitriding of austenitic stainless steel. Surf Coat Technol 2005;195: 81–4.
[11] Shen L, Wang L, Wang Y, Wang C. Plasma nitriding of AISI 304 austenitic stainless steel with pre-shot peening. Surf Coat Technol 2010;204:3222–7.
[12] Hashemi B, Rezaee Yazdi M, Azar V. The wear and corrosion resistance of shot peened-nitrided 316L austenitic stainless steel. Mater Des 2011;32:3287–92.
[13] Tong WP, Tao NR, Wang ZB, Lu J, Lu K. Nitriding iron at lower temperatures. Science 2003;299:686–8.
[14] Tong WP, Liu CZ, Wang W, Tao NR, Wang ZB, Zuo L, et al. Gaseous nitriding of iron with a nanostructured surface layer. Scr Mater 2007;57:533–6.
[15] Kikuchi S, Nakahara Y, Komotori J. Fatigue properties of gas nitrided austenitic stainless steel pre-treated with fine particle peening. Int J Fatigue 2010;32: 403–10.
[16] http://www.mahr.de (accessed October 2012).
[17] UNI 3964. Mechanical testing of metallic materials. Fatigue testing at room temperature, general principles; 1985.
[18] Hassani-Gangaraj SM, Guagliano M. Microstructural evolution during nitriding, finite element simulation and experimental assessment. Appl. Surf. Sci. 2013;271:156–63.
[19] UNI 11153-2. Measurement of thickness of hardened surface layers on ferrous parts. Nitriding and ferritic nitrocarburizing; 2006.
[20] Ashrafizadeh F. Influence of plasma and gas nitriding on fatigue resistance of plain carbon (Ck45) steel. Surf Coat Technol 2003;174–175:1196–200.
[21] Bell T, Loh NL. The fatigue characteristics of plasma nitrided three Pct Cr–Mo steel. J Mater Eng Perform 1982;2:232–7.
[22] ISO 4278. Geometrical product specifications (GPS) – surface texture: profile method-terms, definitions and surface texture parameters, 1st ed.; 1997.
[23] Guagliano M, Vergani L. Effect of nitriding on low-cycle fatigue properties. Int J Fatigue 1997;19:67–73.
[24] Limodin N, Verreman Y, Tarfa TN. Axial fatigue of a gas-nitrided quenched and tempered AISI 4140 steel: effect of nitriding depth. Fatigue Fract Eng M 2003;26:811–20.
[25] Hussain K, Tauqir A, Ul Haq A, Khan AQ. Influence of gas nitriding on fatigue resistance of maraging steel. Int J Fatigue 1999;21:163–8.
[26] Komotori J, Shimizu M, Misaka Y, Kawasaki K. Fatigue strength and fracture mechanism of steel modified by super-rapid induction heating and quenching. Int J Fatigue 2001;23:S225–30.
[27] De La Cruz P, Oden M, Ericsson T. Effect of laser hardening on the fatigue strength and fracture of a B–Mn steel. Int J Fatigue 1998;20:389–98.
[28] Kloos KH, Velten E. Konstruction 1984;36:181–8.